Theory of the Dynamic Aspects of Ultracentrifugation[†]

B. J. McNeil[‡] and J. L. Bethune[*,§]

ABSTRACT: Computer generated concentration distributions have allowed the development of numerical techniques for the determination of sedimentation and diffusion coefficients from the integrated Lamm equation; they are applicable to two component systems with minimal dependence of the characteristic parameters on concentration. Accuracy is assessed by comparison of the *numerically* estimated values of the relevant functions with their *analytical* values, as predicted by the analytical solution of the Mason–Weaver equation. These methods theoretically allow simultaneous calculation of s and D to within 0.5% for a wide range of computer simulated data. The effects of solute heterogeneity on the results are also detailed.

By their very nature, transport processes are dynamic, involving concentration changes in both time and space, the changes being determined by the molecular parameters governing transport in a given experimental system. Thus, for sedimentation in a sector-shaped cell with an imposed radially dependent field, concentration changes with respect to time are related to those with respect to space by the Lamm (1929) equation

$$\frac{\partial c}{\partial t}\bigg|_r = \frac{1}{r}\frac{\partial}{\partial r}\bigg|_t \left\{ Dr\frac{\partial c}{\partial r} - s\omega^2 r^2 c \right\} \qquad (1a)$$

which, on differentiation of the right side, yields, if s and D are not functions of c

$$\frac{\partial c}{\partial t}\bigg|_r = \frac{1}{r}\left\{ Dr\frac{\partial^2 c}{\partial r^2}\bigg|_t + D\frac{\partial c}{\partial r}\bigg|_t - s\omega^2 r^2\frac{\partial c}{\partial r}\bigg|_t - 2s\omega^2 cr \right\} \qquad (1b)$$

where c is the concentration at time t and position r, r is the distance in centimeters from the center of rotation, ω is the angular velocity in radians per second, s is the sedimentation coefficient in seconds, and D is the diffusion coefficient in squared centimeters per second.

For constant ω, values of the derivatives, $\partial c/\partial t|_r$, $\partial c/\partial r|_t$, $\partial^2 c/\partial r^2|_t$, and of c at radius r and time t, *i.e.*, $c(r,t)$, are determined by the local values of s and D; conversely, their determination allows calculation of the s and D pertaining at r.

An integral formulation of eq 1a

$$\int_{r_1}^{r_2} r(\partial c/\partial t)dr = \left\{ Dr\frac{\partial c}{\partial r} - s\omega^2 r^2 c \right\}\bigg|_{r_1}^{r_2} \qquad (2)$$

similarly relates concentration changes *i.e.*, either accumulation or depletion of mass, over a finite segment of the liquid column between r_1 and r_2 to the parameters s and D. It has been proposed that this formulation would allow simultaneous experimental determination of s and D (Archibald, 1947, 1963; Bethune, 1970). The chief advantage of use of eq 2 rather than eq 1b is that integration has removed the necessity of estimating the second derivative of concentration with respect to distance, a process involving significantly higher errors. Since the limits of the integral in eq 2 are not functions of time, it may be reformulated (Sokolnikoff and Redheffer, 1958) as

$$\frac{d}{dt}\int_{r_1}^{r_2} crdr = \left\{ Dr\frac{\partial c}{\partial r} - s\omega^2 r^2 c \right\}\bigg|_{r_1}^{r_2} \qquad (3)$$

Values of s and D are generally concentration (*i.e.*, distance) dependent and, therefore, D and s at r_1 will differ from those at r_2. If, however, the concentration dependence of these parameters may be approximated as $s = s_0(1 - k_s c)$ and $D = D_0(1 - k_D c)$, then eq 3 becomes

$$\frac{d}{dt}\int_{r_1}^{r_2} crdr = \left\{ D_0(1 - k_D c)r\frac{\partial c}{\partial r} - s_0(1 - k_s c)\omega^2 r^2 c \right\}\bigg|_{r_1}^{r_2} \qquad (4a)$$

The resulting equation contains four unknowns, s_0, D_0, k_D, and k_s. Selection of four different pairs of r_1 and r_2 yields four simultaneous equations which allow determinations of these unknowns (Bethune, 1970).[1]

If, however, k_s and k_D are small, that is, if s and D are minimally dependent on concentration, eq 3, in the limit of $k_s = k_D = 0$, reduces to eq 4b

$$\frac{d}{dt}\int_{r_1}^{r_2} crdr = \left\{ D_0\frac{\partial c}{\partial r} - s_0\omega^2 r^2 c \right\}\bigg|_{r_1}^{r_2} \qquad (4b)$$

containing only two unknowns and requiring choice of two pairs of r_1 and r_2 for solution for s_0 and D_0.

[1] Equation 4a allows values of s and D to be obtained from four simultaneous equations which apply to the same time and the same field but differ in the bounds of integration, or to different times but with the same fields and bounds of integration, or, lastly, to the same time and the same bounds of integration but with different fields. The first approach would appear, *a priori*, to be more accurate than the second, involving as it does observations made at only one time and, in the context of the experimental situation employed here (McNeil and Bethune, 1973), eliminates errors from plate misalignment. The third situation requires either two separate experiments or identification of the concentration distribution present *during* variation of the field within *one* experiment.

As a first development of the use of this approach in transport experiments, this paper details selection of appropriate numerical techniques for application of eq 4b to experimental situations. These techniques were developed using a synthetic datum base generated by computer. A companion paper (McNeil and Bethune, 1972) details the experimental application of the techniques.

Theory

In general, development of numerical techniques applicable to experimental situations is facilitated if different approaches can be first evaluated using appropriately generated synthetic data. Thus, for example, to examine the applicability of techniques for numerical differentiation to sedimentation analysis, error-free concentration profiles, as functions of both time and space, i.e., $c(r,t)$, can serve as the generating matrix of appropriate data for such differentiation. Moreover, if the data are generated from an analytical solution of the appropriate continuity equation, *analytical* values of the derivatives themselves can be calculated to serve as criteria of accuracy of *numerical* estimates. The effects of random errors upon the procedures developed can then be investigated using the same synthetic data.

Appropriate values of $c(r,t)$ for such evaluation applied to sedimentation analysis can be generated from the analytical solution of the Mason–Weaver equation (1924) for sedimentation in a rectangular cell in a uniform force field (Yphantis and Waugh, 1956; LaBar, 1966; Charlwood, 1967).

The relevant equation is

$$\frac{\partial c}{\partial t} = D\frac{\partial^2 c}{\partial r^2} - \omega^2 \bar{r} s \frac{\partial c}{\partial r} \tag{5}$$

where s and D are assumed not to be concentration dependent and therefore equal s_0 and D_0 and where $\bar{r}$ is some mean position, generally the distance of the center of the column from the center of rotation.

The solution can be expressed (Mason and Weaver, 1924) as a Fourier series, suitable for computer applications as

$$\frac{c}{c_0} = \frac{e^{y/\alpha}}{\alpha(e^{1/\alpha} - 1)} + 4\alpha e^{(2y-\tau)/4\alpha} \times$$
$$\sum_{m=1}^{\infty} \frac{A_m(\sin (m\pi y) + 2\pi m\alpha \cos (m\pi y))e^{-m^2\pi^2\alpha\tau}}{(1 + 4m^2\pi^2\alpha^2)^2} \tag{6}$$

where $\tau = s\omega^2 t\bar{r}/(r_b - r_m)$, r_m = radial position of the air–liquid meniscus, r_b = radial position of the base of liquid column, $\alpha = D/[s\omega^2\bar{r}(r_b - r_m)]$, $y = (r - r_m)/(r_b - r_m)$, $A_m = 4m\pi\alpha\{1 - (-1)^m e^{-1/2\alpha}\}$, and c_0 = initial concentration. This equation yields c/c_0 for defined values of y, α, τ (or of their dimensioned components).

Several algebraic manipulations of eq 6 may be performed to simplify evaluation. $e^{y/\alpha}$ may be factored out to yield

$$\frac{c}{c_0} = e^{y/\alpha}\left\{\frac{1}{\alpha(e^{1/\alpha} - 1)} + 4\alpha e^{(-2y-\tau)/4\alpha} \times \right.$$
$$\left.\sum_{m=1}^{\infty} \frac{A_m(\sin (m\pi y) + 2\pi m\alpha \cos (m\pi y))e^{-m^2\pi^2\alpha\tau}}{(1 + 4m^2\pi^2\alpha^2)^2}\right\} \tag{7}$$

Since ω can assume large values, $e^{1/\alpha}$ can attain values larger

than can be readily handled in a computer. Therefore, $1/(e^{1/\alpha} - 1)$ is best reexpressed as an infinite series

$$\frac{1}{(e^{1/\alpha} - 1)} = \sum_{j=1}^{\infty} e^{-j/\alpha} \tag{8}$$

Substitution of eq 8 in eq 7 yields, after taking natural logarithms

$$\ln\left(\frac{c}{c_0}\right) = \frac{y}{\alpha} + \ln\left\{\frac{1}{\alpha}\sum_{j=1}^{\infty} e^{-j/\alpha} + 4\alpha e^{(-2y-\tau)/4\alpha} \times \right.$$
$$\left.\sum_{m=1}^{\infty} \frac{A_m(\sin (m\pi y) + 2\pi m\alpha \cos (m\pi y))e^{-m^2\pi^2\alpha\tau}}{(1 + 4m^2\pi^2\alpha^2)^2}\right\} \tag{9}$$

Values of c are then calculated from

$$c = c_0 e^B \tag{10}$$

where B is the right side of eq 9.

The concentrations calculated at the meniscus and base from eq 9 and 10 can be compared with those obtained from a much simpler form which obtains at these positions. Thus, at the meniscus, $y = 0$, and substitution in eq 6 yields after simplification

$$\frac{c_m}{c_0} = \frac{1}{\alpha(e^{1/\alpha} - 1)} + 8\pi\alpha^2 e^{-\tau/4\alpha}\sum_{m=1}^{\infty} \frac{mA_m e^{-m^2\pi^2\alpha\tau}}{(1 + 4m^2\pi^2\alpha^2)^2} \tag{11a}$$

which for computation may be cast into

$$\frac{c_m}{c_0} = \frac{1}{\alpha}\sum_{j=1}^{\infty} e^{-j/\alpha} + 8\pi\alpha^2 e^{-\tau/4\alpha}\sum_{m=1}^{\infty} \frac{mA_m e^{-m^2\pi^2\alpha\tau}}{(1 + 4m^2\pi^2\alpha^2)^2} \tag{11b}$$

At the base $y = 1$ and

$$\frac{c_b}{c_0} = \frac{e^{1/\alpha}}{\alpha(e^{1/\alpha} - 1)} + 8\pi\alpha^2 e^{(2-\tau)/4\alpha}\sum_{m=1}^{\infty} \frac{m(-1)^m A_m e^{-m^2\pi^2\alpha\tau}}{(1 + 4m^2\pi^2\alpha^2)^2} \tag{12a}$$

which similarly may be written as

$$\frac{c_b}{c_0} = \frac{1}{\alpha}\left\{1 + \sum_{j=1}^{\infty} e^{-j/\alpha}\right\} + 8\pi\alpha^2 e^{(2-\tau)4\alpha} \times$$
$$\sum_{m=1}^{\infty} \frac{m(-1)^m A_m e^{-m^2\pi^2\alpha\tau}}{(1 + 4m^2\pi^2\alpha^2)^2} \tag{12b}$$

Equations 11b and 12b are considerably simpler than eq 6, all the sine and cosine terms in eq 6 having been reduced to either 0 or ± 1; they provided an alternative method for the calculation of c_m and c_b and served as an independent numerical check of the use of eq 9 and 10 for this purpose.

Formulation of Analytical Expressions for Derivatives. To achieve the objective of this development, the Mason–Weaver equation was integrated to give

$$\frac{d}{dt}\int_{r_1}^{r_2} c\,dr = \left.\left\{D\frac{\partial c}{\partial r} - s\omega^2\bar{r}c\right\}\right|_{r_1}^{r_2} \tag{13}$$

Analytical expressions for the necessary functions required for determination of s and D from these equations were obtained from the solution of the Mason–Weaver equation as follows.

Differentiation of eq 6 with respect to τ yields

$$\frac{\partial c/c_0}{\partial \tau} = 4\alpha\pi e^{(2y-\tau)/4\alpha}\left\{-4\alpha^2\pi^2\sum_{m=1}^{\infty}\frac{m^2 F_1 F_2 F_3}{F_4{}^2} - \sum_{m=1}^{\infty}\frac{F_1 F_2 F_3}{F_4{}^2}\right\} \tag{14}$$

where $F_1 = m[1 - (-1)^m e^{-1/2\alpha}]$, $F_2 = e^{-m^2\pi^2\alpha\tau}$, $F_3 = \sin(m\pi y) + 2m\pi\alpha\cos(m\pi y)$, and $F_4 = 1 + 4m^2\pi^2\alpha^2$. Equation 14 can be converted to the measured variable t since

$$\frac{\partial c}{\partial t} = \frac{l}{\omega^2 s\bar{r}}\frac{\partial c}{\partial \tau} \tag{15a}$$

where $l = r_b - r_m$.

$$\frac{\partial c}{\partial t} = \frac{\tau}{t}\frac{\partial c}{\partial \tau} \tag{15b}$$

Differentiation of eq 6 with respect to y yields, after simplification

$$\frac{\partial c/c_0}{\partial y} = \frac{e^{y/\alpha}}{\alpha^2(e^{1/\alpha} - 1)} + 8\pi\alpha e^{(2y-\tau)/4\alpha}\left\{2\alpha \sum_{m=1}^{\infty}\frac{F_2 F_1}{F_4{}^2} \times (m\pi\cos(m\pi y) - 2\pi^2\alpha m^2\sin(m\pi y)) + \sum_{m=1}^{\infty}\frac{F_1 F_2 F_3}{F_4{}^2}\right\} \tag{16}$$

Transformation to the dimensioned variable r can be performed since

$$\frac{\partial c}{\partial y} = l\frac{\partial c}{\partial r} \tag{17a}$$

$$\frac{\partial c}{\partial r} = \frac{1}{l}\frac{\partial c}{\partial y} \tag{17b}$$

The integral in eq 13 may be represented as

$$\int_{y_1}^{y_2} cdy = c_0\left\{\frac{e^{y_2/\alpha} - e^{y_1/\alpha}}{(e^{1/\alpha} - 1)} + 8\alpha^2 e^{-\tau/4\alpha} \times \sum_{m=1}^{\infty}\frac{A_m e^{-m^2\pi^2\alpha\tau}}{(1 + 4m^2\pi^2\alpha^2)^2}\{e^{-y_2/2\alpha}\sin(m\pi y_2) - e^{-y_1/2\alpha}\sin(m\pi y_1)\}\right\} \tag{18a}$$

While this rather cumbersome expression can be simplified if the bounds of integration chosen are $y_1 = 0$ and $y_2 = 1$ (i.e., the meniscus and base, respectively), the value of the integral becomes c_0 and differentiation with respect to time yields zero. These expressions, however, are derived to serve as criteria for evaluation of numerical techniques, and, in general terms, it is difficult to attach significance to deviations from zero. This difficulty may be obviated by consideration of the integral $\int_0^1 cydy$, which may be obtained from eq 6 by cross multiplication by y. If the following substitutions are then made in eq 6

$$a = \frac{1}{2\alpha}$$

$$b = m\pi$$

$$c_0 = 1$$

then after much simplification it can also be shown that

$$\int_0^1 cydy = \frac{1}{2a(e^{2a} - 1)}\{e^{2a}(2a - 1) + 1\} - \sum_{m=1}^{\infty}\frac{8b^2 a}{(a^2 + b^2)^3}(1 - (-1)^m\cosh(a))e^{\frac{-(a^2 + b^2)\tau}{2a}} \tag{18b}$$

Its first derivative with respect to τ is

$$\frac{d}{d\tau}\int_0^1 cydy = \sum_{m=1}^{\infty}\frac{4b^2}{(a^2 + b^2)^2} \times (1 - (-1)^m\cosh(a))e^{\frac{-(a^2 + b^2)\tau}{2a}} \tag{19a}$$

$$\frac{d}{dt}\int_0^1 cydy = \frac{\tau}{t}\frac{\partial}{\partial\tau}\int_0^1 cydy \tag{19b}$$

Conversion back to the experimentally measured space variable, r, is accomplished through the relationship

$$\int_{r_m}^{r_b} crdr = r_m l + l^2\int_0^1 cydy \tag{20}$$

Development of Equations for Use with Synthetic Data. The simultaneous equations considered for data generated by the Mason-Weaver solution are

$$\frac{d}{dt}\int_{r_1}^{r_2} cdr = D\left\{\frac{\partial c}{\partial r_2} - \frac{\partial c}{\partial r_1}\right\} - s\omega^2\bar{r}\{c_2 - c_1\} \tag{21a}$$

$$\frac{d}{dt}\int_{r_3}^{r_4} cdr = D\left\{\frac{\partial c}{\partial r_4} - \frac{\partial c}{\partial r_3}\right\} - s\omega^2\bar{r}\{c_4 - c_3\} \tag{21b}$$

Since each of the four bounds of integration can be evaluated at a large number of locations in the liquid column, it will be convenient to alter the notation for the bounds from r_i, where $1 \leq i \leq 4$, to r_{ij} where $1 \leq i \leq 4$ and $1 < j \leq n$ where n is the number of positions at which the concentration was determined. Thus, $r_{1,3}$ denotes the lower bound of integration in the first of the paired equations and represents the distance of the third position from the center of rotation. For a given i a large number of values of j are accessible. Optimally, variation in the bounds should be performed so that the experimentally determined coefficients of the right side of eq 21a are significantly different from their counterparts in eq 21b, *i.e.*, that the determinant of the matrix of these coefficients differs from zero. Similarly the left sides of the two equations should also be significantly different.

If, for $i = 2$, j is chosen such that $\partial c/\partial r_{2,j} = 0$, *e.g.*, in the plateau, then the paired equations immediately simplify to

$$\frac{d}{dt}\int_{r_{1,j}}^{r_{2,j}} cdr = D\left\{-\frac{\partial c}{\partial r_{1,j}}\right\} - s\omega^2\bar{r}\{c_2 - c_1\} \tag{22a}$$

$$\frac{d}{dt}\int_{r_{3,j}}^{r_{4,j}} cdr = D\left\{\frac{\partial c}{\partial r_{4,j}} - \frac{\partial c}{\partial r_{3,j}}\right\} - s\omega^2\bar{r}\{c_4 - c_3\} \tag{22b}$$

The errors involved in numerical evaluation of the coefficients in eq 22a have now been decreased since one numerical derivative has been eliminated and one of the concentrations, c_2, is

the plateau concentration which can be determined with high accuracy.

Criteria for selection of $r_{1,j}$, $r_{3,j}$, and $r_{4,j}$ remain to be developed. Identities can exist between two of these three variables. Thus, if $r_{3,j} = r_{2,j}$, the accuracy in determination of the first coefficient of eq 22b will be improved in a way identical with that seen in eq 22a. However, such a selection will result in integration in eq 22a and 22b over two independent short segments of the column; on the average the length will be one-half the total column length depending on the location of the plateau. To reduce error, integration and subsequently differentiation over at least one longer interval proved to be desirable, and hence $r_{3,j}$ should differ from $r_{2,j}$. If, in $r_{1,j}$, j is selected near the meniscus, if $r_{1,j} = r_{3,j}$, and, if, in $r_{4,j}$, j is selected near the base, then for the first equation integration will be performed over less than half the column height (if $r_{2,j}$ is near the beginning of the plateau), and for the second equation integration will be performed over nearly the whole column.

It now remains to determine the ranges j can assume for $r_{1,j}$ (and by identity, $r_{3,j}$), and for $r_{4,j}$. Optical artifacts can cause large errors in evaluation of concentrations near the menisci. It has been shown (LaBar, 1966) that such errors are minimized if readings are performed no closer to the menisci than 0.015 cm. Thus, the lower limit for $r_{1,j}$ should be r_m + 0.015 cm and the upper limit for $r_{4,j}$ should be r_b − 0.015 cm. The upper limit for $r_{1,j}$ and the lower limit for $r_{4,j}$ are evaluated by consideration of the choice of $r_{2,j}$. Measurements of concentrations at these locations should be significantly different from such measurements made at $r_{2,j}$. The maximum value of j in $r_{1,j}$ is chosen so that the concentration difference between the concentration obtaining at $r_{1,j}$ and that at the plateau is twice the anticipated error in plate reading. A similar consideration applies to the choice of the minimum value of j in $r_{4,j}$.

Several alternative expressions can be derived from both eq 2 and 13 to minimize the effects of experimental errors and optical artifacts at the menisci. They will be illustrated here using eq 2 as the parent equation. For simplification of presentation the notation r_{ij} will be reduced to r_i with the implicit understanding that each r_i takes on values consistent with the development above.

The equations for a sector shaped cell analogous to those for a rectangular cell, eq 22a and 22b, are

$$\frac{d}{dt}\int_{r_1}^{r_2} crdr = D\left\{-r_1\frac{\partial c}{\partial r_1}\right\} - s\omega^2\left\{r_2{}^2c_2 - r_1{}^2c_1\right\} \quad (23a)$$

$$\frac{d}{dt}\int_{r_3}^{r_4} crdr = D\left\{r_4\frac{\partial c}{\partial r_4} - r_3\frac{\partial c}{\partial r_3}\right\} - s\omega^2\left\{r_4{}^2c_x - r_3{}^2c_3\right\} \quad (23b)$$

If D is eliminated and $r_1 = r_3$, then s can be obtained from

$$s\omega^2 = \frac{\left(r_1\frac{\partial c}{\partial r_1}\right)\frac{d}{dt}\int_{r_1}^{r_4} crdr + \left(r_4\frac{\partial c}{\partial r_4} - r_1\frac{\partial c}{\partial r_1}\right)\frac{d}{dt}\int_{r_1}^{r_2} crdr}{(r_1{}^2c_1 - r_4{}^2c_4)\left(r_1\frac{\partial c}{\partial r_1}\right) + (r_1{}^2c_1 - r_2{}^2c_2)\left(r_4\frac{\partial c}{\partial r_4} - r_1\frac{\partial c}{\partial r_1}\right)} \quad (24)$$

Equation 24 involves integration over one short and one long interval. D can then be obtained from the substitution of eq 24 in either eq 23a or 23b. On the other hand, if eq 24 is altered by splitting the integration in the numerator from r_1 to r_4

to that from r_1 to r_2 plus that from r_2 to r_4 and the resulting expression simplified, calculation for s takes the form

$$s\omega^2 = \frac{\left(r_1\frac{\partial c}{\partial r_1}\right)\frac{d}{dt}\int_{r_2}^{r_4} crdr + \left(r_4\frac{\partial c}{\partial r_4}\right)\frac{d}{dt}\int_{r_1}^{r_2} crdr}{r_4(r_1{}^2c_1 - r_2{}^2c_2)\frac{\partial c}{\partial r_4} + r_1(r_2{}^2c_2 - r_4{}^2c_4)\frac{\partial c}{\partial r_1}} \quad (25)$$

Here integration is performed over two short intervals. Substitution of eq 25 in eq 23a yields the following expression for D

$$D = \frac{-(r_2{}^2c_2 - r_4{}^2c_4)\frac{d}{dt}\int_{r_1}^{r_2} crdr - (r_2{}^2c_2 - r_1{}^2c_1)\frac{d}{dt}\int_{r_2}^{r_4} crdr}{r_4(r_1{}^2c_1 - r_2{}^2c_2)\frac{\partial c}{\partial r_4} + r_1(r_2{}^2c_2 - r_4{}^2c_4)\frac{\partial c}{\partial r_1}} \quad (26)$$

Equations 25 and 26 are similar in form to those obtained if initially $r_3 \neq r_1$, the integration being performed over two short segments of the total column height.

Improved accuracy with use of eq 25 and 26 might be expected if one of the integrals could be eliminated. This situation could occur, for example, as r_4 approached r_2. If this limit of eq 26 is taken, the right-hand side becomes indeterminate since $\partial c/\partial r_4 \rightarrow \partial c/\partial r_2$ and $\partial c/\partial r_2$ has been chosen in the plateau; application of L'Hospital's rule is necessary. After considerable simplification the following limiting equation results

$$D = \frac{-\frac{d}{dt}\int_{r_1}^{r_2} crdr}{r_1\left(\frac{\partial c}{\partial r_1}\right)} + \frac{(r_2{}^2c_2 - r_1{}^2c_1)\frac{\partial c}{\partial r}\Big|_{r_2}}{2c_2r_1\frac{\partial c}{\partial t_1}} \quad (27)$$

s would then be obtained from eq 25.

Integration over two short invervals would be expected to have a diminished error if physical or mathematical restrictions could be imposed on eq 23a and 23b. One such restriction is immediately apparent. If positions are chosen such that

$$r_2{}^2c_2 - r_1{}^2c_1 = r_4{}^2c_4 - r_3{}^2c_3 \quad (28$$

then solution of eq 23a and 23b yields D (for $\partial c/\partial r_2 \neq 0$) as

$$D = \frac{\frac{d}{dt}\int_{r_1}^{r_2} crdr - \frac{d}{dt}\int_{r_3}^{r_4} crdr}{\left(r_2\frac{\partial c}{\partial r_2} - r_1\frac{\partial c}{\partial r_1}\right) - \left(r_4\frac{\partial c}{\partial r_4} - r_3\frac{\partial c}{\partial r_3}\right)} \quad (29)$$

$$s = \frac{-\frac{d}{dt}\int_{r_1}^{r_2} crdr + D\left\{r_2\frac{\partial c}{\partial r_2} - r_1\frac{\partial c}{\partial r_1}\right\}}{\omega^2\left\{r_2{}^2c_2 - r_1{}^2c_1\right\}} \quad (30)$$

Theoretical Considerations in Development of Numerical Methods of Differentiation and Integration

Differentiation. Most differentiation procedures on a set of tabulated points $(x_i, f(x_i), i = 1, 2, \ldots, n)$ are based on the determination of an appropriate polynomial, trigonometric, or transcendental function, $p(x)$, which can yield the deriva-

tive $p'(x)$ as an approximation to the true derivative $f'(x)$. For the most part, these functions can be generated as either collocation functions (*i.e.*, $p(x)$ fits exactly all data points) or as least-squares functions (*i.e.*, $p(x)$ minimizes

$$\sum_{i=1}^{m}(f(x_i) - p(x_i))^2$$

for m data points $m > (n - 1)$).

Collocating polynomial functions are commonly employed and can be of degree 1 to degree $n - 1$; *i.e.*, the points can be taken two at a time (for $n = 1$), or three at a time (for $n = 2$), up to all n at a time (for a polynomial of degree $n - 1$). For functions of degree 1, *i.e.*, linear fits over two points, the formulation is

$$p(x_i) = ax_i + b \qquad (31a)$$

and one derivative, the first, can be obtained as

$$p'(x_i) = a \qquad (31b)$$

Two sets of values are needed for determination of a and b. If pairs $(x_{i-1}, f(x_{i-1}))$ and $(x_{i+1}, f(x_{i+1}))$ are chosen then an interpolating function, designated Stirling's approximation (Conte, 1965), yields the *central* difference formula

$$p'(x_i) = \frac{f(x_{i+1}) - f(x_{i-1})}{2h}$$
$$\qquad (32a)$$
$$h = (x_{i+1} - x_i)$$

with an associated error varying with the third derivative of $f(x)$, *i.e.*

$$E = \frac{-h^2}{6}f'''(\xi), \ x_{i-1} < \xi < x_{i+1} \qquad (32b)$$

For small h this error usually is smaller than that resulting from other combinations of $(x_i, f(x_i))$ pairs (*e.g.*, x_i, $f(x_i)$ and x_{i+1}, $f(x_{i+1})$ as used in Newton's *forward* difference formula), and differentiation by the central difference formula is preferable when linear interpolation is used.

For higher order polynomials the following formulation is valid

$$p(x) = a + bx + cx^2 + dx^3 \ldots\ldots + wx^n \qquad (33)$$

if $(n + 1)$ tabulated values are available and yields all derivatives up to the nth. The fitting of a second degree polynomial (Conte, 1965) for the numerical determination of second derivatives is commonly employed, yielding an expression analogous to the central difference formula for first derivatives, *i.e.*

$$p''(x_i) = \frac{f(x_{i+1}) - 2f(x_i) + f(x_{i-1})}{h^2} \qquad (34a)$$

Here, the error, E, involves a fourth derivative of $f(x)$, *i.e.*

$$E = \frac{-h^2}{12}f^{iv}(\xi) \qquad (34b)$$

Trigonometric and exponential functions can be used in least-squares numerical differentiation in two ways. The first involves determination of the constants of the appropriate least-squares functions (*e.g.*, those governing a Fourier series or those governing the sum of several exponentials (Hartley, 1961)) with derivatives following from differentiation of the relevant formulation. Alternatively, numerical linear differentiation formulae (*vide supra*) can be modified to allow their use with nonlinear data. If $A[f(x_i)]$ is an analytical function which allows linearization of $f(x_i)$, then eq 32a can be reformulated as

$$p'(x_i) = \frac{A[f(x_{i+1})] - A[f(x_{i-1})]}{2h}\frac{1}{A'[f(x_i)]} \qquad (35)$$

Integration. Numerical integration is generally associated with higher accuracy than is numerical differentiation. Most procedures employed are based on the approximation of the continuous function $f(x)$ by an appropriate interpolating polynomial $p(x)$ and on the approximation of numerical summation to analytical integration. Final selection of $p(x)$ is dictated by two considerations: (1) the range over which the tabulated data can be approximated accurately by simple functions, and (2) the magnitude of the truncation error, defined as

$$\int_{x_0}^{x_i} f(x)dx - \int_{x_0}^{x_i} p(x)dx$$

where x_0 and x_i are the bounds of integration. Tabulated values of truncation errors (Scheid, 1968) for interpolating polynomials of degree m with equispaced data points indicate that formulae of degree m for any even m (an odd number of data points) have comparable accuracy to those of the next higher degree, *i.e.*, $m + 1$ (an even number of data points). Thus, for example, Simpson's Quadrature rule for $m = 2$ fitted to the three points, x_0, x_1, and x_2, yields the integral

$$\int_{x_0}^{x_2} f(x)dx = \frac{h}{3}[p(x_0) + 4p(x_1) + p(x_2)] \qquad (36a)$$

For connected quadratic fits over the $(i + 1)$ points, x_0, x_1, x_i, the integral is

$$\int_{x_0}^{x_i} f(x)dx = \frac{h}{3}[p(x_0) + 4p(x_1) + 2p(x_2) +$$
$$\ldots 2p(x_{i-2}) + 4p(x_{i-1}) + p(x_i)] \quad (36b)$$

The Newton-Cote 3/8 formulation for $m = 3$ for fits over four points is

$$\int_{x_0}^{x_3} f(x)dx = \frac{3h}{8}[p(x_0) + 3p(x_1) + 3p(x_2) + p(x_3)] \quad (37)$$

and by analogy with eq 36b a similar expression for connected cubic fits over $(i + 1)$ points can be elaborated. However, these are of no greater accuracy than eq 36a and 36b. The truncation error for these functions varies approximately as $h^5/y^4(\xi)$, where h is the interval between data points and $y^4(\xi)$ the fourth derivative of the interpolating polynomial at an intermediate point ξ in the integrating interval.

Results and Discussion

All calculations were performed using an IBM 360/65 computer with programs written in Fortran IVH or a Sigma-7 time sharing computer with programs written in Fortran II. Single precision was employed throughout. For the IBM 360/65 computer the Scientific Subroutine Library was used where indicated. Hand calculations carried out to four significant figures agreed with the results of computer calculations at that level of accuracy. c_0 was kept constant at 2.5 g/l.

Reexpression of $1/(e^{1/\alpha} - 1)$ in terms of an infinite series (eq 8) provided a convenient and rapid method for evaluation of this expression; the series expansion coverged to one part in the seventh decimal place for $0.01 \leq \alpha \leq 2.7$. The lower limit occurred for $s = 11.3$ S, $D = 4.0$ F, $\bar{r} = 6.94$ cm, $l = 0.18$ cm, speed = 55,000 rpm, and the upper limit for $s = 2.54$ S, $D = 9.5$ F, $\bar{r} = 6.94$ cm, $l = 0.18$ cm, speed = 10,000 rpm.

The second summation term involved in the calculation of c (eq 9) converged with the same accuracy, generally within ten iterations (i.e., $m \leq 10$).

Calculations of c at the meniscus and base by eq 9 and 10 agreed with results obtained from the alternative expressions (eq 11b and 12b) for solution in these locations to one part in the sixth decimal place.

Analytical values of $\partial c/\partial t$, $\partial c/\partial r$, $\int_{r_m}^{r_b} cr dr$, and $d/dt \int_{r_m}^{r_b} cr dr$ (vide supra) served as references for evaluation of numerical techniques used for their approximation. The most important factor determining the overall accuracy of numerical techniques for these functional forms was the magnitude of their absolute values as determined for a given set of pertinent physical parameters by the applied field. Many numerical techniques for a wide range of experimental parameters indicated that good numerical approximations for all of these functional forms could be obtained if

$$10^{-5} < \left|\frac{\partial c}{\partial t}\right|_r \leq 10^{-3} \text{ g/(l. sec)} \qquad (38a)$$

$$10 < \left|\frac{\partial c}{\partial r}\right|_t \leq 10^3 \text{ g/(l. cm)} \qquad (38b)$$

These limits demonstrate that best results were obtained at early times of experimentation before boundary formation. For a rectangular cell in a uniform field these ranges are not independent since

$$\left.\frac{\partial c}{\partial t}\right|_r = \left.\frac{\partial r}{\partial t}\right|_c \left.\frac{\partial c}{\partial r}\right|_t$$

$$\left.\frac{\partial c}{\partial t}\right|_r = -(s\omega^2 \bar{r})\left.\frac{\partial c}{\partial r}\right|_t$$

All of the numerical techniques presented here were obtained from synthetic data fulfilling the above restrictions.[2]

Because of the anticipated need to smooth data in actual experimental situations, techniques were developed for smoothing the concentration arrays generated from the ana-

lytical solution of the Mason–Weaver equation. While it may seem strange to use smoothing techniques on error-free synthetic data, evaluation of the different functional forms and of the technique of smoothing can proceed hand in hand since the usefulness of a simple function in approximating, over a short range, an actual concentration distribution can be measured by the degree of departure of the values predicted by simple functions from those generated by the more complex analytical solution of the continuity equation. Data were smoothed in time rather than in distance in order to minimize the effects of potential errors from plate misalignment in the horizontal plane since these errors would have a significant effect on the determination of $\partial c/\partial t$ and $d/dt \int_{r_1}^{r_2} cr dr$.

Numerical Estimates of $c(r,t)$. To evaluate different functions used in smoothing concentration as a function of time analytical values of $c(r,t)$ were compared with the smoothed numerical values of $c(r,t)$ calculated from appropriate least-squares parameters. Near the centripetal portion of the liquid column, where $\partial c/\partial t < 0$, $c(r,t)$ could be accurately linearized in time with the use of the hyperbolic cotangent of c, i.e., coth (c); near the centrifugal regions of the liquid column where $\partial c/\partial t > 0$, use of coth $(1/c)$ provided equally good linearization. Thus, for the former case, the relation is

$$\coth (c) = a_1 + b_1 t$$

and for the latter

$$\coth (1/c) = a_2 + b_2 t$$

n data points, $n \geq 2$, are required for evaluation of a and b.

Linearization over two intervals or three data points ($n = 3$) proved most satisfactory for evaluation of c. Three independent estimates of c can thus be calculated; i.e., the smoothed value of c can be obtained from use of a smoothing array in which the *unsmoothed* value of c at time j occupies the first position in the array (the other two elements being at $j + \Delta t$ and $j + 2\Delta t$) or the second position (the other two elements being at $j - \Delta t$ and $j + \Delta t$) or the third position (the other two being elements at $j - 2\Delta t$ and $j - \Delta t$).[3] The location that the concentration at time j occupies in the smoothing array is designated k (i.e., $k = 1$, $k = 2$, $k = 3$, respectively, for the above three positions). Table I indicates that for $n = 3$ smoothed and analytical values of $c(r,t)$ agree to within 0.04%, higher values of n leading, on the average, to larger differences between analytical and smoothed values. Variation in the sign of the error in $c(r,t)$ as k is varied from 1 to 3 for $n = 3$ (Table I) suggested that an averaging procedure over k might further improve the accuracy of the procedure. For the first and last times of observation, only one calculated value of concentration is available, and, therefore, averaging cannot be performed. For the second and penultimate times of observation only two calculated values of concentration are available and for these times averaging over two values only was accomplished while for the remaining times averaging can be performed over three values. When $\partial c/\partial t$ was restricted to the range indicated in inequality (eq 38a), this averaging procedure significantly improved the accuracy in prediction of

---

[2] Detailed analyses of methods for evaluation of $\partial c/\partial t$ are not presented since the expression $(d/dt) \int_{r_m}^{r_b} cr dr$ provided a more accurate method for numerical calculations than did $\int_{r_m}^{r_b} (\partial c/\partial t) r dr$ (vide infra). However, elaborate methodology has been developed for optimum numerical evaluation of $\partial c/\partial t$ (McNeil, 1972).

[3] The calculation of three independent values requires separate storage in the computer of the unsmoothed and smoothed values of concentration as a function of position and time.

TABLE I: Per Cent Errors in Calculating Concentrations at the Base by Linear Least Squaring Using $A[f(c)] = \coth(1/c) = a + bt.$[a]

k	n			
	3	5	7	9
1	−0.014	−0.074		
2	+0.033	+0.048		
3	−0.020	+0.100		
4		+0.051		
5		−0.147	+0.163	
6			−0.034	
7			−0.475	
8				−0.330

[a] Because of a limited number of initial analytical values of $c(r,t)$, all entries of the table could not be calculated. Input parameters are: $s = 2.54$ S, $D = 9.5$ F, speed $= 25,000$ rpm, cell length $= 0.18$ cm, $\bar{r} = 6.94$ cm, time $= 900$ sec, $n =$ number of data pairs used for least squaring, and $k =$ location that the concentration at time j occupies in n.

concentration values over the whole liquid column. Resultant errors, i.e.

$$\frac{c_i - c_{\text{true}}}{c_{\text{true}}} \times 100$$

where c_i is the average calculated concentration and c_{true} the analytical value of the concentration were of the order 10^{-2}–$10^{-4}\%$ (Table II).

Numerical Methods for Evaluation of $\partial c/\partial r$. Numerical differentiation in the spatial plane was performed on concentrations smoothed as a function of time as indicated above. Derivatives were calculated as follows

$$\frac{\partial c(r_i,t)}{\partial r} = \frac{\partial c_i}{\partial r} = \frac{c(r_{i+1},t) - c(r_{i-1},t)}{2\Delta r} \quad (39a)$$

$$\frac{\partial c(r_i,t)}{\partial r} = \frac{\partial c_i}{\partial r} = \frac{\ln[c(r_{i+1},t)] - \ln[c(r_{i-1},t)]}{2\Delta r} c(r_i,t) \quad (39b)$$

Δr, defined as $r_{i+1} - r_i$, was finally set at 0.005 cm, being a compromise between increased accuracy of numerical differentiation at smaller values of Δr and increased difficulty of data acquisition.

Analytical values and numerical values for $\partial c/\partial r$ (Table III)

TABLE II: Per Cent Errors in Calculation of Concentration after Least-Squaring Concentration as a Function of Time and Using the Averaging Procedure Described in Text.[a]

Position	600 sec	1000 sec
6.85 cm (meniscus)	−0.48 × 10⁻³	−0.76 × 10⁻⁴
6.91 cm	+0.73 × 10⁻³	−0.12 × 10⁻²
6.97 cm	−0.67 × 10⁻³	+0.31 × 10⁻³
7.03 cm (base)	−0.14 × 10⁻²	−0.66 × 10⁻⁴

[a] Input parameters are: $s = 5$ S, $D = 7$ F, speed $= 25,000$ rpm, cell length $= 0.18$ cm, $\bar{r} = 6.94$ cm, and $\Delta t = 200$ sec.

TABLE III: Calculation of Analytical and Numerical Values of $\partial c/\partial r$ from 300 to 1700 sec; $\Delta t = 200$ sec.[a]

Anal. $\partial c/\partial r$ (g/(l. cm))	% Error in Numerical $\partial c/\partial r$[b]	% Error in Numerical $\partial c/\partial r$[c]
Part a: Near the Meniscus		
21.8132	0.13	−0.35
21.1449	0.18	−0.18
20.3360	0.16	−0.14
19.5478	0.13	−0.13
18.8099	0.12	−0.11
18.1261	0.13	−0.08
17.4936	0.09	−0.11
16.9085	0.10	−0.08
Part b: Near the Base		
31.8233	−0.69	−0.13
35.5046	−0.41	0.04
38.2896	−0.33	0.06
40.6430	−0.29	0.06
42.7396	−0.26	0.06
44.6646	−0.24	0.06
46.4642	−0.23	0.05
48.1637	−0.21	0.05

[a] Input parameters are: $s = 2.54$ S, $D = 7.0$ F, speed $= 25,000$ rpm, $\Delta r = 0.005$ cm, cell length $= 0.18$ cm, and $\bar{r} = 6.94$ cm. [b] Calculated from eq 39a. [c] Calculated from eq 39b.

for one set of input parameters indicate average errors of 1% near both the meniscus (Table IIIa) and base (Table IIIb) where the largest gradients occurred in these simulations; intermediate locations, except in positions where $\partial c/\partial r$ approaches zero, were equally accurate. Moreover, for $\partial c/\partial r \geq$ 30–40 g/(l. cm), eq 39b yielded more accurate results, particularly near the base, than did eq 39a. For values of $\partial c/\partial r$ below 30 g/(l. cm), however, either procedure was equally accurate.

Effects of Random Errors in Data Acquisition on $c(r,t)$ and $\partial c/\partial r$. Before an investigation of more complex numerical procedures, i.e., integration and integration followed by differentiation, was begun, an analysis of the effects of random errors on the approximation of $c(r,t)$ and $\partial c/\partial r$ was made in order to ensure their adequate approximation after introduction of an error of magnitude anticipated experimentally. Since actual experiments were to be performed with currently available Model E ultracentrifuge equipment using Kodak IIg plates, the maximum absolute magnitude of the error in reading was estimated at 5×10^{-4} to 10×10^{-4} cm (Bethune, 1970). The reading errors were assumed to reside only in the measurement of $c(r,t)$ and were assumed to be normally distributed so that any resulting set of error-containing concentrations was normally distributed around the true analytical concentration. Rectangularly distributed numbers (Subroutine Random, Dr. P. J. Lewis) were converted to normally distributed numbers using Hamming's (1962) approximation and a variation of the IBM subroutine GAUSS. Reading errors in centimeters were converted into concentration errors in milligrams.[4] Provisions were made in the computer program

---

[4] For a fringe separation of 0.025 cm and with one fringe corresponding to 0.25 mg/ml, then a reading error of 5×10^{-4} cm corresponds to an error of 0.005 mg/ml.

TABLE IV: Average Per Cent Error in Calculation of $c(r,t)$ as a Function of Cell Location, the Number of Readings, n, and the Maximum Magnitude of the Random Errors, σ, Introduced.[a]

σ (μ)	n		
	1	5	10
At the Meniscus			
5	0.44	0.19	0.11
10	0.88	0.38	0.23
At the Base			
5	0.05	0.02	0.02
10	0.10	0.04	0.03

[a] Input parameters are: s = 5.0 S, D = 7.0 F, speed = 25,000 rpm, $\bar{r}$ = 6.94 cm, and cell length = 0.18 cm.

TABLE V: Comparison of Analytical and Numerical Values of $(d/dt)\int_{r_m}^{r_b} cr \, dr$ Using Error-Free Concentration Arrays.[a]

Time (sec)	Anal. Values $\times 10^5$ (mg/(cm sec))	% Error in Numerical Values
400	0.8397	1.10
600	0.7843	0.83
800	0.7359	0.27
1000	0.6918	−0.02
1200	0.6507	1.80
1400	0.6118	−0.86
1600	0.5746	0.33

[a] Input parameters are: s = 5.0 S, D = 7.0 F, speed = 25,000 rpm, cell length = 0.18 cm, $\bar{r}$ = 6.94 cm, and Δr = 0.005 cm.

to simulate multiple readings of each point by generating and then averaging a series of error-associated concentrations. Table IV summarizes the average errors in $c(r,t)$ obtained over 20 times of observation at the meniscus and base for one set of input parameters and indicates that if multiple readings are simulated, the accuracy of the approximations is improved. Errors in $c(r,t)$ are less than 0.4% if multiple readings are simulated. Similar improvement occurs in the evaluation of $\partial c/\partial r$, multiple readings reducing the error in many cases to the level of the error-free systems themselves in all positions except those in and near the plateau where $\partial c/\partial r$ approaches or is zero.

Methods for Numerical Integration. Since numerical evaluation of $\partial c/\partial r$ had been successful over a range encompassing three data points or two intervals, each of length Δr, polynomials of degree m = 2 and 3 were selected for use as interpolating functions in studies of numerical integration. The IBM subroutine QSF provided a convenient technique for integrating over an area with either an even or odd number of data points using a combination of Simpson's quadrature rule and the Newton–Cote 3/8 formula. The same increment of Δr, 0.005 cm, used for numerical estimates of $\partial c/\partial r$ was used for these integration procedures. Analytical and numerical values of $\int_{r_m}^{r_b} cr \, dr$ were compared, the analytical value having been calculated according to eq 18b and the numerical value resulting from use of QSF. The agreement between analytical and numerical values was excellent, usually to within one part in 10^5 whenever the ranges of $\partial c/\partial t$ and $\partial c/\partial r$ were restricted to those already indicated (*vide supra*). This technique for numerical integration was so highly accurate that no other techniques were examined.

The effects of maximum errors of 5×10^{-4} or 10×10^{-4} cm, in either a single reading or in averages over five or ten readings, on areas determined by numerical integration were studied. The smoothing effects of numerical quadrature were apparent even when the reading was performed only once with a maximum error of 10×10^{-4} cm, the resulting error generally being less than one part in 10^3.

Evaluation of techniques for estimation of $\int_{r_m}^{r_b}(\partial c/\partial t)r \, dr$ (or equivalently of $(d/dt)\int_{r_m}^{r_b} cr \, dr$ (Sokolnikoff and Redheffer, 1958)) revealed that, in the former case, *i.e.*, in integration of an expression involving $\partial c/\partial t$, accurate results were obtained only when analytical values of $\partial c/\partial t$ were used, best error-free numerical approximations of $\partial c/\partial t$ giving large errors (>10%)

in the resulting integral. However, use of the other formulation and application of the central difference formula for numerical differentiation yielded errors of the order of 1% (Table V) when error-free smooth concentrations were used in the integrand. Despite this excellent approximation with error-free data it was assumed that the addition of an experimental error would markedly reduce the accuracy of numerical estimates particularly since the value of the integral is small and relatively insensitive to time. And, indeed, a maximum 5×10^{-4} cm error averaged over five readings increased the average error to over 15%. This insensitivity is not unexpected. The largest concentration changes with time occur, in the context of our experimental design, at and near the menisci, the effects in these locations being approximately equal in magnitude but opposite in sign. Thus the inclusion of areas near both the meniscus and base in the integration procedure produces a near-zero change in the integral with time (Table V) while exclusion of one of these regions should yield integrals with larger time derivatives and resulting decreased sensitivity to experimental errors.

To assess numerical procedures evaluated between any r_i and r_j it was necessary to develop reference values. Such values were obtained by multiplying *analytical* values of $\partial c/\partial t$ by r and then integrating the product over the *entire* liquid column; the results closely approximate those obtained from

TABLE VI: Analytical and Near-Analytical Values of $\int_{r_m}^{r_b}(\partial c/\partial t) \cdot r \, dr$ Using Error-Free Data and Analytical Values of $\partial c/\partial t$.[a]

Time (sec)	First Temporal Derivatives ($\times 10^5$) (mg/(cm sec))	
	Anal. (eq 19b)	Near Anal.
400	0.8397	0.8387
600	0.7843	0.7837
800	0.7359	0.7355
1000	0.6918	0.6916
1200	0.6507	0.6505
1400	0.6118	0.6116
1600	0.5746	0.5744

[a] Input parameters are: s = 5.0 S, D = 7.0 F, speed = 25,000 rpm, cell length = 0.18 cm, $\bar{r}$ = 6.94 cm, and Δr = 0.005 cm.
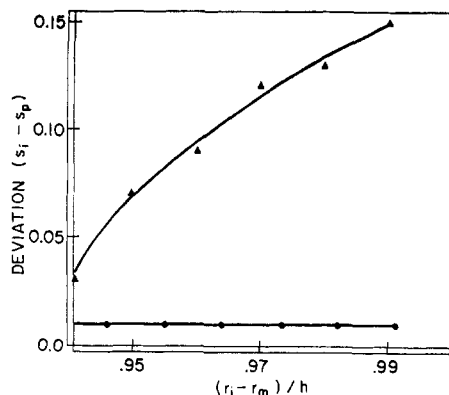
FIGURE 1: Effect of heterogeneity in calculated value of s. For the homogeneous sample $s = 2.54$ S, $D = 9.5$ F; for the heterogeneous sample a 50:50 mixture of two macromolecular components was assumed with $s = 2.54$ and 5.0 S and $D = 9.5$ and 7.0 F. The ordinate represents the deviation of the value calculated at point r_i from 2.54 S for the homogeneous sample and 3.77 S for the heterogeneous sample. The abscissa represents increasing distances, i.e., increasing upper limits of integration, along the liquid column from the center of rotation, starting at r_m and normalized to the total height of the column, h.
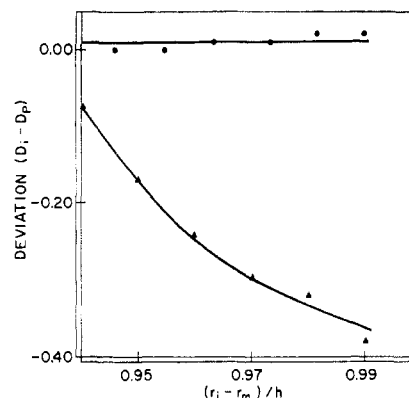
FIGURE 2: Effect of heterogeneity in calculated value of D. For the homogeneous sample $s = 2.54$ S, $D = 9.5$ F; for the heterogeneous sample a 50:50 mixture of two macromolecular components was assumed with $s = 2.54$ and 5.0 S and $D = 9.5$ and 7.0 F. The ordinate represents the deviation of the value calculated at point r_i from 9.5 F for the homogeneous sample and 8.25 F for the heterogeneous sample. The abscissa represents increasing distances, i.e., increasing upper limits of integration, along the liquid column from the center of rotation, starting at r_m and normalized to the total height of the column, h.

the complex analytical expression (eq 19b) derived from solution of the Mason–Weaver equation (Table VI). Similar results should obtain for integration between any r_i and r_j.

In an attempt to obtain larger values for the time derivative of the integral, studies were made with the region near the meniscus excluded from the integral. Thus, for readings obtained every 50 μ, $i = 3$, and the time derivative becomes $(d/dt) \int_{r_3}^{r_j} cr dt$. As expected (Table VII) for many values of j near the base of the liquid column the magnitude of the derivative is 100 times greater than that found when integration is performed over the whole column (Table VI). Moreover the introduction of a maximum 5×10^{-4} cm error averaged over five readings leads to an error of only 1%; this effect is not dependent on time.

Because excellent approximations for all of the functional forms necessary for solution of eq 13 were obtained both in

the absence of an experimental error and in the presence of an appropriate experimental error averaged over several sets of readings, these techniques were then applied to an error-free data base to test the accuracy of eq 13 for solution for s and D. Table VIII illustrates values of s and D calculated from several pairs of simultaneous equations using input physical parameters appropriate to chymotrypsinogen. For these calculations the bounds of integration for each member of the pair of simultaneous equations followed the analysis above: i.e., $r_{2,j}$ was chosen as a location in the plateau; $r_{1,j} = r_{3,j}$ where j was selected near the air–solution meniscus; for $r_{4,j} j$ was selected near the base. For all combinations of bounds the agreement between input and calculated values of s and D is excellent, within 0.5% for both parameters.

Further calculations with the introduction of experimental errors into the concentration matrix were not performed be-

TABLE VII: Per Cent Errors in Numerical[a] Estimates of $(d/dt) \cdot \int_{r_i}^{r_j} cr dr$ Using as Reference Near-Analytical[b] Values of $\int_{r_i}^{r_j} (\partial c/\partial t) r dr$; $i = 3$ and $3 < j \leq 37$, where $i = 1$ Corresponds to the Meniscus and $j = 37$ to the Base.[c]

j	Near-Anal. Values $(\times 10^3)$	% Diff in Numerical Estimates
4	−0.2934	0.76
12	−0.2654	0.57
20	−0.3503	0.58
28	−0.3281	0.60
36	−0.0281	−0.04
37	+0.0574	1.66

[a] Calculated in the presence of a maximum experimental error of 5×10^{-4} cm averaged over five readings. [b] Calculated in the absence of an experimental error and using analytical values of $\partial c/\partial t$. [c] Input parameters are: $s = 5.0$ S, $D = 7.0$ F, $\Delta r = 0.005$ cm, $\bar{r} = 6.94$ cm, cell length = 0.18 cm, speed = 25,000 rpm, time = 800 sec, and $\Delta t = 100$ sec.

TABLE VIII: Effect of Varying the Bounds of Integration in Equations 21a and 21b in the Calculation of the Sedimentation and Diffusion Coefficients.[a]

Values of j in $r_{1,j}$	Values of j in $r_{4,j}$	Calcd Values of s and D					
		107	108	109	110	111	112
2		2.55	2.55	2.55	2.54	2.54	2.54
		9.48	9.49	9.49	9.50	9.50	9.50
3		2.55	2.55	2.54	2.54	2.54	2.54
		9.48	9.49	9.49	9.49	9.50	9.50
4		2.55	2.54	2.54	2.54	2.54	2.54
		9.48	9.48	9.49	9.49	9.50	9.50
5		2.54	2.54	2.54	2.54	2.54	2.53
		9.48	9.48	9.49	9.49	9.49	9.50
6		2.54	2.54	2.54	2.54	2.53	2.53
		9.47	9.48	9.48	9.49	9.49	9.49

[a] Input parameters are: $s = 2.54$ S, $D = 9.50$ F, speed = 24,000 rpm, $\bar{r} = 6.94$ cm, cell length = 0.56 cm, $\Delta r = 0.005$ cm, time = 1200 sec, and $\Delta t = 200$ sec.

cause of the computational difficulties associated with accurately approximating the experimental situation which solution by eq 2 and 13 is designed to minimize, *i.e.*, the varying magnitude of the errors at the menisci.

The success of this calculation procedure, *i.e.*, variation of the bounds of integration in the evaluation of s and D, suggested its use in the detection of sample heterogeneity. Since separation by sedimentation leads to accumulation of the heavier component at the bottom of the cell, differences in calculated values of s and D might be expected as r_4 is varied, r_1, r_2, and r_3 remaining constant. To test this hypothesis simulation of a three component system was performed by calculating independently the concentration arrays for each of two macromolecular species and then obtaining the total concentration at position r and time t, *i.e.*, $c(r,t)$ from

$$c(r,t) = \sum_{i=1}^{2} c_i(r,t)$$

Figures 1 and 2 compare results obtained for one such 50:50 mixture at one time of experimentation with those for a homogeneous sample (*vide supra*); bounds of integration were selected with the restrictions indicated above. At all times as r_4, the upper bound of integration of the second integral, approaches the base the calculated value of s increases (Figure 1) and that of D decreases (Figure 2).

Homogeneous samples exhibiting a variation of s with concentration, *i.e.*

$$s = s_0(1 - k_s c)$$

should exhibit a different pattern of calculated values of s; for

large values of k_s and/or a large increase in concentration at the base, calculated values of s should decrease as r_4 approaches the base of the liquid column.

References

Archibald, W. J. (1947), *J. Phys. Colloid Chem. 51*, 1204.

Archibald, W. J. (1963), *in* Ultracentrifugal Analysis, Williams, J. W., Ed., New York, N. Y., Academic Press, pp 37–46.

Bethune, J. L. (1970), *Biochemistry 9*, 2745.

Charlwood, P. A. (1967), *Biopolymers 5*, 663.

Conte, S. D. (1965), Elementary Numerical Analysis, New York, N. Y., McGraw-Hill Book Company.

Hamming, R. W. (1962), Numerical Methods for Scientists and Engineers, New York, N. Y., McGraw-Hill Book Company, pp 34 and 389.

Hartley, H. O. (1961), *Technometrics 3* (2), 269.

LaBar, F. E. (1966), *Biochemistry 5*, 2362.

Lamm, O. (1929), *Z. Physik. Chem. A143*, 177.

Mason, M., and Weaver, W. (1924), *Phys. Rev. 23*, 412.

McNeil, B. J. (1972), Ph.D. Dissertation, Harvard University, Cambridge, Mass.

McNeil, B. J., and Bethune, J. L. (1973), *Biochemistry 12*, 3254.

Scheid, F. (1968), Numerical Analysis, New York, N. Y., McGraw-Hill Book Company, Schaum's Outline Series, p 111.

Sokolnikoff, I. S. and Redheffer, R. M. (1958), Mathematics of Physics and Modern Engineering, New York, N. Y., McGraw-Hill Book Company.

Yphantis, D. A., and Waugh, D. F. (1956), *J. Phys. Chem. 60*, 623.